

SU(3) centre vortices underpin confinement and dynamical chiral symmetry breaking

Elyse-Ann O'Malley, Waseem Kamleh, Derek Leinweber, and Peter Moran
*Centre for the Subatomic Structure of Matter (CSSM),
 School of Chemistry & Physics, University of Adelaide 5005, Australia*

The mass function of the nonperturbative quark propagator in $SU(3)$ gauge theory shows only a weak dependence on the vortex content of the gauge configurations. Of particular note is the survival of dynamical mass generation on vortex-free configurations having a vanishing string tension. This admits the possibility that mass generation associated with dynamical chiral symmetry breaking persists without confinement. In this paper we examine the low-lying ground state hadron spectrum of the π , ρ , N and Δ and discover that while dynamical mass generation persists in the vortex-free theory, it is not connected to dynamical chiral symmetry breaking. In this way, centre vortices in $SU(3)$ gauge theory are intimately linked to both confinement and dynamical chiral symmetry breaking.

PACS numbers: 12.38.Gc 11.15.Ha 12.38.Aw

I. INTRODUCTION

Numerical simulations of QCD on a space-time lattice reveal that the essential, fundamentally important, non-perturbative features of the QCD vacuum fields are:

1. The dynamical generation of mass through chiral symmetry breaking (χ SB), and
2. The confinement of quarks.

However, there exists no derivation of quark confinement starting from first principles, nor is there a totally convincing explanation of the effect.

The questions that dominate the field centre around gaining an understanding on how these fundamentally important features of QCD come about. The question is: *What is the essence of QCD vacuum structure?* That is, what is it about the field fluctuations of the QCD vacuum that causes quarks to be confined? What aspects of the QCD vacuum are responsible for dynamical mass generation? Do the underlying mechanisms share a common origin?

The prevailing view is that quark confinement and dynamical χ SB is the work of some special class of gauge field configurations which dominate the QCD vacuum on large distance scales. Candidates have included instantons, Abelian monopoles, and centre vortices. In recent years, algorithms have been invented which can locate these types of objects in thermalized lattices, generated by the lattice Monte Carlo technique. This is an important development enabling *ab initio* investigations of the underlying mechanism of quark confinement and dynamical χ SB.

Instantons are natural candidates to explain χ SB as each instanton is associated with a zero mode of the Dirac operator [1]. An accumulation of zero eigenvalues will produce a quark condensate [2]. However, instantons are no longer favored to play a significant role in confinement [3].

An attractive mechanism for confinement is dual superconductivity of the QCD vacuum [4, 5]. The con-

densation of chromo-magnetic monopoles has been observed directly after gauge-fixing to “Maximal Abelian Gauge” [6], from which the idea of “Abelian dominance” has emerged. There, the Abelian degrees of freedom of the Yang-Mills field are thought to encode all its long-distance properties. However, degrees of freedom more elementary than Abelian monopoles, embedded in them and solely responsible for the physics assigned to them, cannot be ruled out [7].

Like Abelian dominance, centre vortices are exposed by gauge-fixing. Usually, a gauge transformation is applied which brings each lattice link as close as possible to a centre element of the gauge group. The centre of a group is that set of group elements which commute with all other elements of the group. For an $SU(N)$ gauge group, the centre elements consist of all $g \in SU(N)$ proportional to the $N \times N$ unit matrix, \mathbf{I} , subject to the condition that $\det(g) = 1$. This is the set of N $SU(N)$ group elements $\{Z_m\}$, with

$$Z_m = \exp\left(i\frac{2\pi}{N}m\right)\mathbf{I}, \quad (m = 0, 1, 2, \dots, N-1). \quad (1)$$

These centre elements form a discrete Abelian subgroup known as Z_N . Vortices are identified as the defects in the centre-projected gauge field. Again, the idea of centre dominance is that the centre degree of freedom encodes all the long-distance nonperturbative physics.

In $SU(2)$ gauge theory, a clear link between centre vortices, confinement and mass generation via dynamical chiral symmetry breaking is manifest [8]. Centre vortices are the single underlying mechanism giving rise to both chiral symmetry breaking and quark confinement in $SU(2)$ gauge theory.

Whether this is the case for the $SU(3)$ Yang-Mills theory relevant to QCD is not as clear. As outlined in Refs. [9–11] the relation between centre vortices and dynamical chiral symmetry breaking is much more complicated in $SU(3)$ gauge theory. Ref. [11] explores the role of centre vortices identified by gauge fixing Monte Carlo generated configurations to maximal centre gauge [12],

clearly illustrating how dynamical mass generation survives the removal of these vortices. This admits the possibility that the underlying mechanisms generating confinement and dynamical chiral symmetry breaking are decoupled.

We proceed to investigate the low-lying hadron mass spectrum in this unique centre-vortex-free environment lacking confinement and retaining dynamical mass generation. A brief report on this was presented at Lattice 2011 [13]. Our aim here is to search for evidence of dynamical chiral symmetry breaking and thus provide further insight into the role of centre vortices in QCD.

II. CENTRE VORTICES

There are multiple methods of identifying centre vortices, such as the Maximal Centre Gauge [14–16] and Laplacian Centre Gauge [17] with various preconditioning options [18]. Here we focus on vortices identified by gauge fixing the original Monte-Carlo generated configurations directly to Maximal Centre Gauge without any preconditioning. This is the same identification used in Ref. [11], which revealed the survival of dynamical mass generation on such vortex-free configurations.

First the links $U_\mu(x)$ are gauge transformed to be brought close to the centre elements of $SU(3)$,

$$Z = \exp\left(2\pi i \frac{m}{3}\right) \mathbf{I}, \text{ with } m = -1, 0, 1. \quad (2)$$

On the lattice this is implemented by searching for the gauge transformation Ω such that,

$$\sum_{x,\mu} |\text{tr } U_\mu^\Omega(x)|^2 \xrightarrow{\Omega} \max. \quad (3)$$

One can then project the gluon field to a centre-vortex only configuration where each link is a number (one of the roots of unity) times the identity matrix

$$U_\mu(x) \rightarrow Z_\mu(x) \text{ where } Z_\mu(x) = \exp\left(2\pi i \frac{m_\mu(x)}{3}\right) \mathbf{I}, \quad (4)$$

where $m_\mu(x) = -1, 0, 1$.

The vortices are identified by the centre charge, z , found by taking the product of the links around a plaquette,

$$z = \prod_{\square} Z_\mu(x) = \exp\left(2\pi i \frac{n}{3}\right). \quad (5)$$

If $z = 1$, no vortex pierces the plaquette. If $z \neq 1$ a vortex with charge z pierces the plaquette. In the smooth gauge-field limit, all the links approach the identity, and no vortices are found. It is only when we get a non-trivial change of phase around the plaquette that a vortex is identified.

Vortices are removed by removing the centre phase. This is done by making the transformation

$$U_\mu(x) \rightarrow U'_\mu(x) = Z_\mu^*(x) U_\mu(x). \quad (6)$$

In $SU(2)$ gauge theory the removal of the centre vortices results in a lack of string tension which is fully recovered in the vortex-only configurations. The mass function of the nonperturbative quark propagator observed in the vortex-removed configurations is flat and shows no sign of dynamical mass generation.

The findings in $SU(3)$ gauge theory[11] differ from the $SU(2)$ case. While the removal of centre vortices removes the string tension, the string tension is not fully recovered in the vortex-only configurations. An examination of the mass function of the nonperturbative quark propagator reveals only small differences in dynamical mass generation between the original and vortex-removed configurations. This shape indicates the retention of dynamical mass generation, despite the absence of confinement. This leads to the key question under investigation. Is the persistence of dynamical mass generation a manifestation of dynamical chiral symmetry breaking in the absence of confinement?

We note that at large momenta, the mass function of the propagator of the vortex-removed configurations experiences a vertical shift upwards of approximately 60 MeV for a given bare quark mass. This may be attributed to a roughening of the configurations at short distances associated with the removal of centre vortices via Eq. 6.

III. RESULTS

To further investigate the underlying physics, we calculate the standard effective masses for low-lying hadrons from their Euclidean two-point functions. We compare the effective masses for the π , ρ , N and Δ hadrons obtained from the regular and vortex-removed configurations for varying quark masses. Our uncertainties are obtained via the jackknife analysis with best fits obtained through a consideration of the full covariance-matrix based χ^2 per degree of freedom.

A statistical ensemble of 200 $SU(3)$ gauge-field configurations is generated using the Lüscher-Weisz [19] mean-field improved action on a $20^3 \times 40$ lattice with a lattice spacing of 0.125 fm. We use the FLIC fermion action [20] providing nonperturbative $\mathcal{O}(a)$ improvement [21] with improved chiral properties allowing efficient access to the light quark-mass regime [22].

Initially we consider four different values for the Wilson hopping parameter, κ , selected to provide a wide view of the mass dependence of the spectrum. We consider $\kappa = 0.1280, 0.1293, 0.1304$ and 0.1310 . The associated quark mass can be estimated by linearly extrapolating the squared pion mass to zero as a function $1/\kappa$. The critical hopping parameter κ_{cr} is the value at which pion mass vanishes, such that

$$m_q = \frac{1}{2a} \left(\frac{1}{\kappa} - \frac{1}{\kappa_{\text{cr}}} \right). \quad (7)$$

We first examine the pion effective mass as a function of Euclidean time. The mass for each κ is plotted in figure

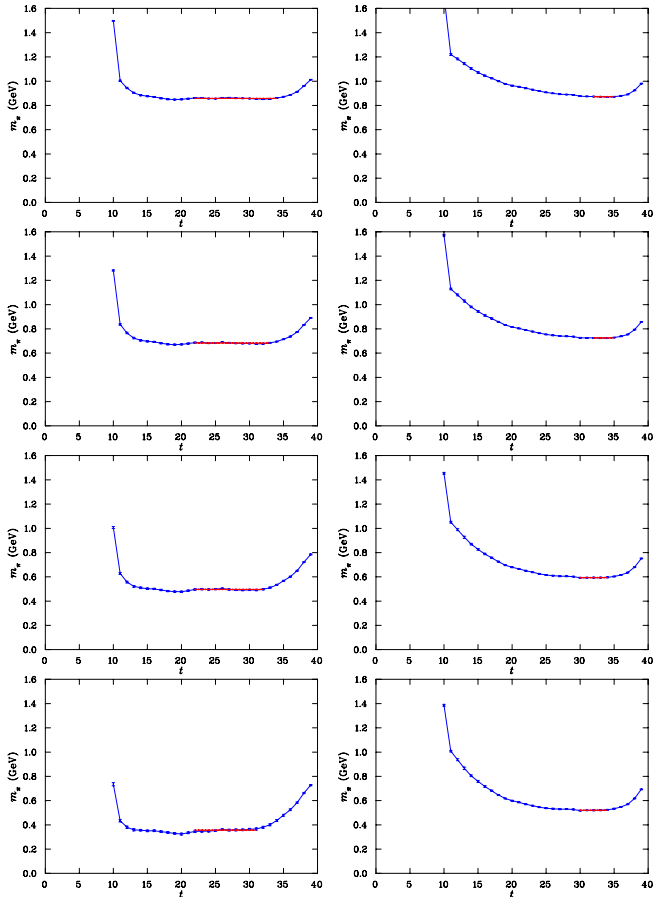


FIG. 1: Comparison of the pion effective mass evolution $m(t)$ for the original configurations (left) and the vortex-free configurations (right) as the quark mass is decreased from the top downwards. The values of the hopping parameter κ are 0.1280 (top), 0.1293, 0.1304 and 0.1310 (bottom).

1, where the left column shows the normal configurations and the right shows the vortex-free configurations.

The pion results reveal an important difference between the two sets of configurations in the approach to the mass plateau. The plateau is approached rapidly on the original configurations, indicating the presence of a significant mass gap between the ground state and the first excited state excited by the standard pseudoscalar interpolating field. In contrast the approach to the plateau on the vortex-free configurations is slow, suggesting a tower of closely spaced pion excitations. Indeed the shape is reminiscent of the free-field two-point correlator where excitations are associated with free quarks having back-to-back momenta of increasing values. These phenomena are also observed for the ρ -meson effective-mass evolution presented in Fig. 2.

In the case of the pion, the effective masses from the vortex-free configurations sit much higher than the regular masses; they do not show the same low mass associated with the pseudo Goldstone boson of QCD.

An examination of the pion masses of the vortex-

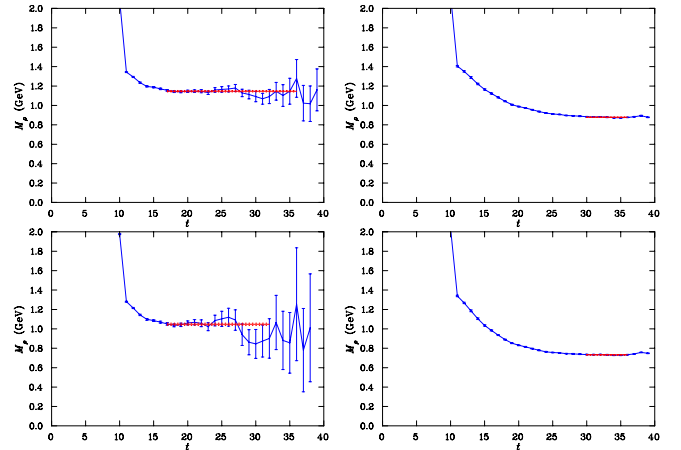


FIG. 2: Comparison of the ρ -meson effective mass evolution $m(t)$ for the original configurations (left) and the vortex-free configurations (right) as the quark mass is decreased from the top downwards. The values of the hopping parameter κ are 0.1280 (top) and 0.1293 (bottom).

removed configurations as a function of the inverse hopping parameter in Fig. 3 reveals that it is possible to perform simulations at hopping parameters smaller than the κ_{cr} obtained from the original configurations. This is in accord with Ref. [11], where the mass function for the vortex-removed configurations is shifted higher by about 60 MeV indicating smaller bare quark masses are required to obtain the same renormalised quark mass. We consider two additional hopping parameter values for the vortex-free configurations which are unphysical for the normal configurations. We take $\kappa = 0.1320$, and 0.1325.

This necessarily leads to a different κ_{cr} for the vortex-free configurations when using Wilson-style fermions. Taking the lightest three masses and assuming $m_\pi^2 \propto 1/\kappa$ in the vortex-free theory provides the linear extrapolation and vortex-free κ_{cr} illustrated in Fig. 3. Note that the heavier quark masses in the vortex-free theory show a clear deviation from linear behaviour.

Of course an alternative scenario is also possible. One could argue that dynamical chiral symmetry breaking is spoiled in the vortex-free theory with m_π^2 no longer proportional to $1/\kappa$ or m_q . When a quark of mass zero is placed in the vortex-removed configurations, the pion still has mass. A comparison of the π and ρ meson masses will reveal the correct scenario.

In Fig. 4 the pion mass from the original and vortex-free configurations is plotted as a function of the bare quark mass, m_q (determined with reference to the critical κ value from the original configurations). While it seems the vortex-free mass will approach zero as the quark mass decreases, the relationship between the quark mass and m_π is evidently different between the original and vortex-free configurations.

The Gell-Mann-Oakes-Renner relationship, $m_\pi^2 \propto m_q$ can be seen in the results from the original configurations

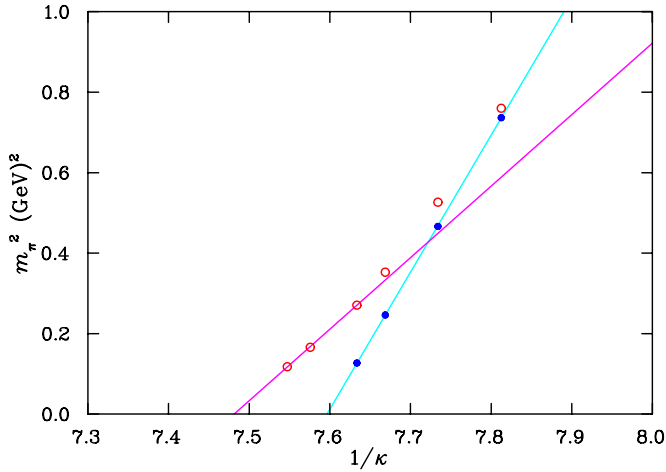


FIG. 3: Pion mass squared in terms of the inverse hopping parameter, κ^{-1} . The lines illustrate fits to the original configurations and the vortex-free configurations, the latter addressing only the lightest three quark masses considered where there is some promise that $m_\pi^2 \propto \kappa^{-1}$.

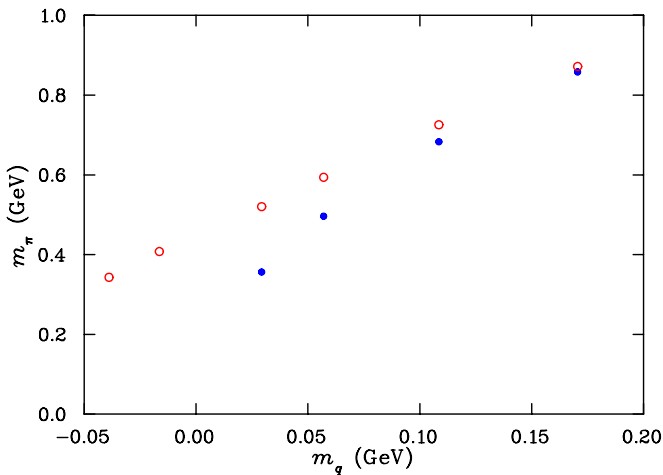


FIG. 4: Pion mass in GeV as a function of the bare quark mass determined with reference to the original configurations. Full symbols illustrate results from the original configurations while the open symbols illustrate results from the vortex-free configurations.

as the points have the shape of a typical square-root function. While the pion masses obtained in the vortex-free configurations at the two lightest quark masses considered are of a similar magnitude to that of the lightest pion mass from the original configurations, there is no evidence of the curvature associated with $m_\pi^2 \propto m_q$.

In the vortex-free configurations the data appears linear with $m_\pi \propto m_q$ over a wide range of m_q , indicating a significant difference between the two types of configurations and a loss of the Goldstone nature of the pion in the vortex-free theory.

The ground-state masses for the pion on the regular and vortex-removed configurations are summarised

in Table I.

TABLE I: π -meson masses from the original and vortex-free ensembles as a function of the hopping parameter, κ . The quark mass, m_q is determined with reference to the original Monte Carlo generated configurations. Units are GeV as applicable.

κ	m_q	Original m_π	Vortex-free m_π
0.1280	0.1705	0.8582(17)	0.8717(29)
0.1293	0.1085	0.6830(19)	0.7256(32)
0.1304	0.0570	0.4963(24)	0.5939(28)
0.1310	0.0293	0.3564(34)	0.5204(29)
0.1320	-0.0164	unphysical	0.4077(38)
0.1325	-0.0389	unphysical	0.3431(43)

TABLE II: ρ -meson masses from the original and vortex-free ensembles as a function of the hopping parameter, κ . The quark mass, m_q is determined with reference to the original configurations. Units are GeV as applicable.

κ	m_q	Original m_ρ	Vortex-free m_ρ
0.1280	0.1705	1.146(8)	0.8781(23)
0.1293	0.1085	1.047(12)	0.7326(23)
0.1304	0.0570	0.982(16)	0.6058(23)
0.1310	0.0293	0.933(29)	0.5350(24)
0.1320	-0.0164	unphysical	0.4128(37)
0.1325	-0.0389	unphysical	0.3492(39)

This loss of a pseudo-Goldstone boson in the vortex-free theory becomes very clear once one compares the masses of the π and ρ mesons in the vortex-free theory. Table II reports ρ -meson masses and Fig. 5 illustrates masses for the π and ρ mesons obtained from the original configurations (full symbols) and the vortex-free configurations (open symbols). This figure clearly illustrates how the π and ρ mesons become nearly degenerate on the vortex-free configurations. Thus the vortex-free pion is not associated with dynamical chiral symmetry breaking. It is not a pseudo-Goldstone boson.

The degeneracy of the π and ρ meson is somewhat surprising. For example, in a simple quark model the ρ -meson mass sits much higher than that of the pion due to a large hyperfine interaction between the quark and anti-quark. The degeneracy of the masses on the vortex-removed configurations implies that any hyperfine interactions have also been removed with the removal of the centre vortices.

Turning our attention to the baryon sector, the nucleon and Δ are presented in Fig. 6 for both the original and the vortex-free configurations. From this graph we

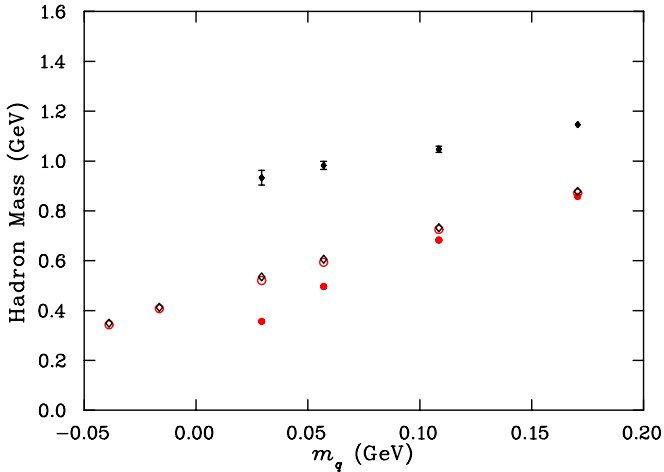


FIG. 5: Masses for the π (circles) and ρ (diamonds) mesons obtained from the original configurations (full symbols) and the vortex-free configurations (open symbols).

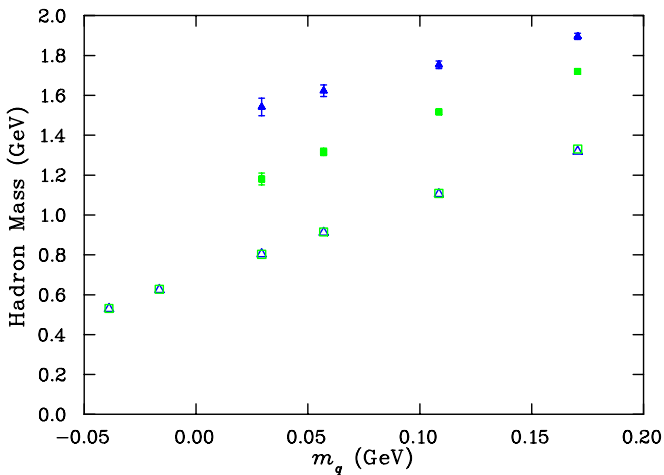


FIG. 6: Masses of the Δ (triangles) and N (squares) from the original gauge-field configurations are compared with the masses from the vortex-free configurations. Full symbols illustrate results from the original configurations while the open symbols illustrate results from the vortex-free configurations.

see that the vortex-free masses for the N and Δ are approximately degenerate, similar to the case of the ρ and π mesons. Again we see the absence of hyperfine interactions in the vortex-free theory. Moreover, both baryons have much lower masses in the vortex-free theory. Numerical values for the N and Δ are provided in Tables III and IV respectively.

To view the entire hadron mass spectrum we have investigated, all the hadron masses are plotted on the same axes in Fig. 7. While hadron masses have become degenerate within the meson and baryon sectors, it is important to note that significant dynamical mass generation is occurring. The dynamical mass generation observed in the quark mass function of the nonperturbative quark propagator is also manifest here.

TABLE III: Nucleon masses from the original and vortex-free ensembles as a function of the hopping parameter, κ . The quark mass, m_q is determined with reference to the original configurations. Units are GeV as applicable.

κ	m_q	Original m_N	Vortex-free m_N
0.1280	0.1705	1.720(12)	1.3309(43)
0.1293	0.1085	1.517(14)	1.1078(47)
0.1304	0.0570	1.317(19)	0.9150(47)
0.1310	0.0293	1.181(30)	0.8026(48)
0.1320	-0.0164	unphysical	0.6275(53)
0.1325	-0.0389	unphysical	0.5309(56)

TABLE IV: Δ baryon masses from the original and vortex-free ensembles as a function of the hopping parameter, κ . The quark mass, m_q is determined with reference to the original configurations. Units are GeV as applicable.

κ	m_q	Original m_Δ	Vortex-free m_Δ
0.1280	0.1705	1.896(16)	1.3187(48)
0.1293	0.1085	1.753(19)	1.1054(38)
0.1304	0.0570	1.623(29)	0.9118(39)
0.1310	0.0293	1.542(44)	0.8043(39)
0.1320	-0.0164	unphysical	0.6251(45)
0.1325	-0.0389	unphysical	0.5298(46)

Consider for example, hadron masses at the heaviest quark mass, as this value has the most accuracy. Here, the input quark mass is 0.17 GeV. In a free theory, the meson mass would be 0.34 GeV and the baryon mass would be 0.51 GeV. These values are much less than the measured masses of 0.87 GeV and 1.32 GeV for the meson and baryon sectors respectively, indicating that whilst the particles have become degenerate, dynamical mass generation is still present.

The mass generation is reminiscent of the early constituent-quark model where current quarks are thought to be dressed by QCD-vacuum interactions giving rise to a constituent quark mass. This is done in a model that does not have a connection to chiral symmetry.

The apparent degeneracy of the masses from the vortex-free configurations indicates perhaps that the hadron mass being measured is merely the sum of the dressed constituent-quark-like masses of the quarks composing the hadron. Taking into account the number of constituent quarks composing each hadron, Fig. 8 illustrates the masses of the pion, rho meson, 2/3 of the nucleon mass and 2/3 of the Delta mass as a function of quark mass. This graph reveals all four hadrons having the same mass in the vortex-free theory after one ac-

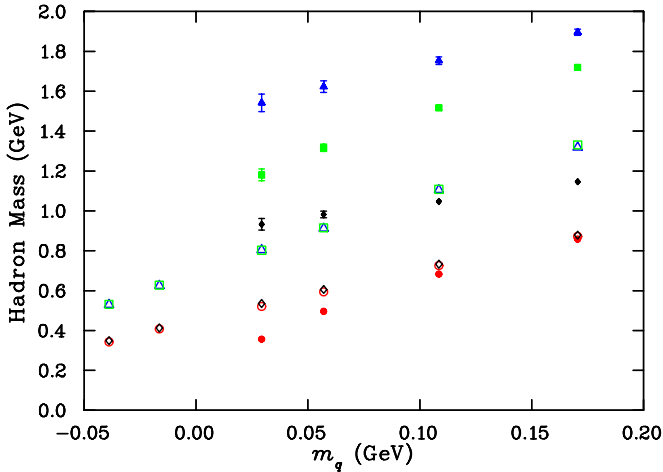


FIG. 7: Low-lying hadron mass spectrum obtained from the original configurations (full symbols) and the vortex-free configurations (open symbols). The symbols correspond to the various hadrons considered. For the original configurations, from lowest to highest hadron masses, the symbols correspond to π , ρ , N and Δ .

counts for the number of quarks required to compose the quantum numbers of the state. The vortex-free theory is simply a theory of weakly interacting constituent quarks.

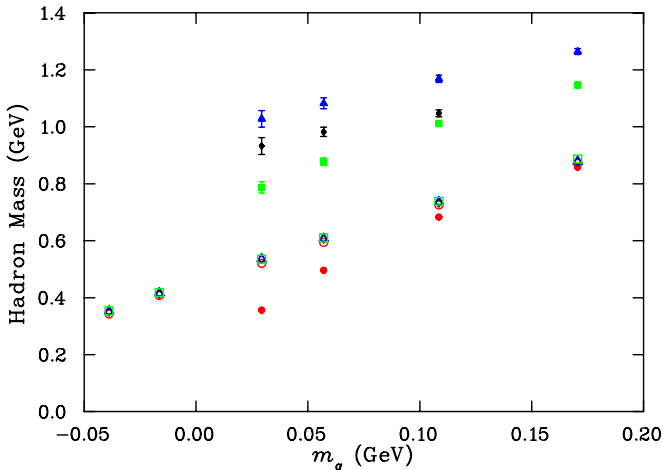


FIG. 8: The low-lying meson mass spectrum is compared with the low-lying baryon mass spectrum multiplied by $2/3$ to account for the number of constituent quarks composing the system. Results from the original configurations (full symbols) and the vortex-free configurations (open symbols) are illustrated. The symbols are as in Fig. 7.

The absence of interactions to lift the degeneracy of the states is somewhat unexpected. While the static quark potential loses confinement in the vortex-free theory, the short distance, Coulomb-like interactions persist. Indeed it is the associated one-gluon-exchange interactions that motivated the spin-dependent interactions such as spin-orbit or spin-spin hyperfine interactions of early quark models. And while these hadron masses have been cal-

culated in an environment which retains the Coulombic part of the potential there is no evidence of the associated spin-dependent interactions. Either, the short-distance noise introduced in the process of centre-vortex removal has spoiled these short-distance interactions or the dominant origin of spin-dependent interactions is in the confining part of the potential.

IV. CONCLUSIONS

This study resolves an important question on the role of centre vortices in dynamical chiral symmetry breaking in $SU(3)$ gauge theory. Is the persistence of dynamical mass generation in the mass function of the quark propagator a manifestation of dynamical chiral symmetry breaking in the absence of confinement?

Prior to this work, studies of the quark propagator in $SU(3)$ gauge theory [11] admitted the possibility that the underlying mechanisms generating confinement and dynamical chiral symmetry breaking were decoupled as dynamical mass generation survives in the absence of confinement. This work resolves this issue by revealing that the dynamical mass generation observed in the vortex-free theory is not associated with chiral symmetry.

A comparison of the input quark mass and the hadron masses reveals that dynamical mass generation is at work. This is in accord with Ref. [11] which clearly illustrates how dynamical-mass generation survives the removal of centre vortices.

However, of greatest importance is the complete absence of any remnant of dynamical chiral symmetry breaking in the mass spectrum of the vortex-free theory. We find a pion degenerate with the ρ meson and a mass dependence of $m_\pi \propto m_q$ inconsistent with the properties of the pseudo-Goldstone boson of chiral symmetry. Because these key results are drawn from the vortex-free theory alone the results are robust, independent of any uncertainty in defining the critical hopping parameter in the vortex-free theory.

From our calculations of the hadron mass spectrum, we have seen that the hadron masses of the vortex-free theory are simply a reflection of the number of quarks required to compose their quantum numbers. There is little evidence of quark interactions in the mass spectrum and this is in accord with the general features of the Euclidean time evolution of the hadron effective masses in the vortex-free theory where the spectrum suggests a theory of free constituent quarks.

One interesting question which remains is the nature of the vortex-free hadron spectrum at vanishing quark mass. To explore this question one must adopt a fermion action for which the chiral limit is well defined at $m_q = 0$. For example, both staggered and overlap fermion formalisms provide this property and it would be interesting to further examine the vortex-free spectrum with these actions.

In conclusion, centre vortex removal spoils both confinement and chiral symmetry. Centre-vortices are the

most fundamental degrees of freedom in QCD, essential to confinement and dynamical chiral symmetry breaking. Just as in $SU(2)$, there is an intimate relationship between centre vortices, confinement and dynamical chiral symmetry breaking. Both confinement and dynamical chiral symmetry breaking are lost under centre vortex removal.

Acknowledgments

It is a pleasure to acknowledge the contributions of Kurt Langfeld and Alan Ó Cais in centre gauge fixing

and centre projecting the gauge field configurations [18] used in this study. This research was undertaken on the NCI National Facility in Canberra, Australia, which is supported by the Australian Commonwealth Government. We also acknowledge eResearch SA for grants of supercomputing time. This research is supported by the Australian Research Council.

-
- [1] G. 't Hooft, Phys.Rev. **D14**, 3432 (1976).
 - [2] T. Banks and A. Casher, Nucl.Phys. **B169**, 103 (1980), revised Version.
 - [3] D. Chen, R. Brower, J. W. Negele, and E. V. Shuryak, Nucl.Phys.Proc.Suppl. **73**, 512 (1999), hep-lat/9809091.
 - [4] G. 't Hooft, Nucl. Phys. **B190**, 455 (1981).
 - [5] S. Mandelstam, Phys.Rept. **23**, 245 (1976).
 - [6] H. Shiba and T. Suzuki, Phys.Lett. **B333**, 461 (1994), hep-lat/9404015.
 - [7] P. de Forcrand and M. D'Elia, Phys. Rev. Lett. **82**, 4582 (1999), hep-lat/9901020.
 - [8] P. O. Bowman, K. Langfeld, D. B. Leinweber, A. O' Cais, A. Sternbeck, et al., Phys.Rev. **D78**, 054509 (2008), 0806.4219.
 - [9] D. Leinweber, P. Bowman, U. Heller, D. Kusterer, K. Langfeld, et al., Nucl.Phys.Proc.Suppl. **161**, 130 (2006).
 - [10] A. O. Cais, W. Kamleh, B. Lasscock, D. Leinweber, L. von Smekal, et al., PoS **LAT2007**, 321 (2007), 0710.2958.
 - [11] P. O. Bowman, K. Langfeld, D. B. Leinweber, A. Sternbeck, L. von Smekal, et al., Phys.Rev. **D84**, 034501 (2011), 1010.4624.
 - [12] L. Del Debbio, M. Faber, J. Giedt, J. Greensite, and S. Olejnik, Phys.Rev. **D58**, 094501 (1998), hep-lat/9801027.
 - [13] E.-A. O'Malley, W. Kamleh, D. Leinweber, and P. Moran, PoS **LATTICE 2011**, 257 (2011).
 - [14] L. Del Debbio, M. Faber, J. Greensite, and S. Olejnik, Phys. Rev. **D55**, 2298 (1997), hep-lat/9610005.
 - [15] K. Langfeld, H. Reinhardt, and O. Tennert, Phys. Lett. **B419**, 317 (1998), hep-lat/9710068.
 - [16] K. Langfeld, Phys. Rev. **D69**, 014503 (2004), hep-lat/0307030.
 - [17] P. de Forcrand and M. Pepe, Nucl. Phys. **B598**, 557 (2001), hep-lat/0008016.
 - [18] A. O' Cais, W. Kamleh, K. Langfeld, B. Lasscock, D. Leinweber, et al., Phys.Rev. **D82**, 114512 (2010), 0807.0264.
 - [19] M. Lüscher and P. Weisz, Commun. Math. Phys. **97**, 59 (1985).
 - [20] J. M. Zanotti et al. (CSSM Lattice Collaboration), Phys.Rev. **D65**, 074507 (2002), hep-lat/0110216.
 - [21] J. Zanotti, B. Lasscock, D. Leinweber, and A. Williams, Phys.Rev. **D71**, 034510 (2005), hep-lat/0405015.
 - [22] S. Boinepalli, W. Kamleh, D. B. Leinweber, A. G. Williams, and J. M. Zanotti, Phys.Lett. **B616**, 196 (2005), hep-lat/0405026.